Journal of Macromolecular Science, Part A
Publication details, including instructions for authors and subscription information:
http://www.informaworld.com/smpp/title~content=t713597274

Biodegradable Nanocomposites Based on the Polyester Poly(3-hydroxybutyrate-co-3-hydroxyhexanoate) and Layered Silicate or Expanded Graphite

Xiujuan Zhang[a]; Gui Lin[a]; Reda Abou-Hussein[a]; William M. Allen[b]; Isao Noda[b]; James E. Mark[a]
[a] Department of Chemistry and the Polymer Research Center, The University of Cincinnati, Cincinnati, OH [b] The Procter & Gamble Company, West Chester, OH

Online publication date: 04 January 2011

To cite this Article Zhang, Xiujuan , Lin, Gui , Abou-Hussein, Reda , Allen, William M. , Noda, Isao and Mark, James E.(2008) 'Biodegradable Nanocomposites Based on the Polyester Poly(3-hydroxybutyrate-co-3-hydroxyhexanoate) and Layered Silicate or Expanded Graphite', Journal of Macromolecular Science, Part A, 45: 6, 431 — 439
To link to this Article: DOI: 10.1080/10601320801977624
URL: http://dx.doi.org/10.1080/10601320801977624

Journal of Macromolecular Science®, Part A: Pure and Applied Chemistry (2008) **45**, 431–439

ISSN: 1060-1325 print/1520-5738 online
DOI: 10.1080/10601320801977624

Biodegradable Nanocomposites Based on the Polyester Poly(3-hydroxybutyrate-co-3-hydroxyhexanoate) and Layered Silicate or Expanded Graphite

XIUJUAN ZHANG,[1] GUI LIN,[1] REDA ABOU-HUSSEIN,[1] WILLIAM M. ALLEN,[2] ISAO NODA,[2] and JAMES E. MARK[1]

[1]*Department of Chemistry and the Polymer Research Center, The University of Cincinnati, Cincinnati, OH*
[2]*The Procter & Gamble Company, West Chester, OH*

Received and accepted December, 2007

Novel nanocomposites based on the biodegradable polymer poly(3-hydroxybutyrate-co-3-hydroxyhexanoate) (PHBHx) and layered fillers, specifically layered silicate (clay25A) and expanded graphite (EG), were prepared by melt intercalation. The dispersion of the fillers in the PHBHx was characterized by wide-angle X-ray diffraction (WAXD) and transmission electron microscopy (TEM). The effects of the fillers on the polymer structure, thermal stability and mechanical properties of the nanocomposites were also studied, by differential scanning calorimetry, thermogravimetric analysis, and strain-stress measurements in elongation, respectively. The WAXD and TEM results showed that the clay25A and EG was exfoliated into well-dispersed sheets in the polymer matrix, especially when the filler concentration were relatively low. This gave rise to considerable improvements in Young's modulus, and resulted in increases in the thermal degradation. It should be possible to convert the EG dispersions obtained thus far to ones yielding filler-filler networks that show electrical conductivity.

Keywords: biodegradable polymers; layered silicates; expanded graphite; thermal stability; mechanical properties

1 Introduction

Nowadays, biodegradable polymers are becoming an important research focus (1–3), since they can be degraded by bioactive environments (such as those containing bacteria, fungi, or algae), or by hydrolysis in sea water or even buffer solutions. For this reason, such polymers can be used as attractive substitutes for many synthetic materials, thereby alleviating problems associated with solid waste disposal. Worldwide consumption of biodegradable polymers increased from 14 million kg in 1996 to an estimated 68 million kg in 2001.

Poly(3-hydroxyalkanoates) (PHA), a class of biodegradable and biocompatible polyesters, has in fact attracted much research interest and industrial attention as substitutes for synthetic materials (4–8). These polymers can be produced directly from renewable resources by microbes which accumulate them as carbon and energy storage materials under unbalanced growth conditions. The copolyesters, poly(3-hydroxybutyrate-co-3-hydroxyhexanoate) (PHBHx), are some of the most important biodegradable semi-crystalline aliphatic polyesters in this PHA family. They provide a unique combination of properties such as superior thermo-plasticity, excellent biocompatibility, and biodegradability, etc. (4, 5), and are of interest for disposable packaging applications because of their being environmentally benign. However, there is a need for more research for achieving improvements in the mechanical, thermal stability and barrier properties (to water and gases) when these PHBHx materials are applied in more widespread areas (7, 8). One feasible method, described in some of our previous studies, applies the technique of orientation induced by pre-stretching to improve the mechanical properties of polymers (9, 10). Another relevant method is the preparation of hybrids made of PHBHx and inorganic materials; such hybrids may circumvent these limitations on PHBHx, and thereby expand its applications. The general goal would thus be to incorporate an environmentally acceptable filler to improve PHBHx properties relevant to their use as packaging materials.

Incorporation of exfoliated layered silicates to prepare polymer/layered silicate nanocomposites has attracted considerable attention since the earliest work of some Toyota Corporation researchers (11). One of our previous studies

Address correspondence to: James E. Mark, Department of Chemistry, The University of Cincinnati, Crosley Tower, Martin Luther King Drive, Cincinnati, OH 45221-0172. Tel.: +1-513-556-9292; Fax: +1-513-556-9239; E-mail: markje@email.uc.edu

showed that incorporating organically modified clay fillers by solution intercalation improved the mechanical properties of these promising copolyesters (12). In addition to clays, there are exfoliated layered particles such as expanded graphite (EG), a typical pseudo-two-dimensional solid in bulk form (13, 14). Similar to the clays, this EG could also provide very effective reinforcement of polymers at loading levels much smaller than required in the case of solid particles such as carbon black and silica (15–17). Moreover, it is an electrically conductive filler (18–20).

In the present investigation, some biodegradable nanocomposites based on PHBHx and layered fillers, specifically organically modified clay or EG, were prepared by melt blending. The morphology and dispersion of the layered silicates and EG in PHBHx, and their effects on crystallinity, mechanical properties, thermal degradability, and conductivity of these materials were also investigated.

2 Experimental

2.1 Materials

The molecular structure of the PHBHx is shown in Figure 1. A sample was generously provided by Meredian Inc, and used as received. It was a random copolymer consisting of 87–89 mol% 3-hydroxybutyrate, and 11–13 mol% 3-hydroxyhexanoate (based on NMR analysis). It had a number-average molecular weight of 500,000–600,000 g mol^{-1} and a polydispersisty index M_w/M_n of 1.9–2.1 based on polystyrene standards. The layered-silicate was a sample of Cloisite 25A (designed as clay25A), which had been modified with quaternary alkylammonium cations (Figure 2), and was purchased from Southern Clay Products Inc., Gonzales, Texas. The average interlayer distance in clay25A was about 18.6 Å. The graphite flakes had an average size of 500 μm and were used to prepare the EG; they were generously provided by the Asbury Graphite Mills, Inc., Asbury, NJ. Concentrated sulfuric acid and concentrated nitric acid were obtained from Aldrich, and all of these chemicals were used as received, without further purification.

2.2 EG Preparation

The expanded graphite employed was prepared from natural graphite flakes, which are naturally abundant and cheap, composed of aggregates of graphite sheets, 1–2 nm in thickness, and 0.335 nm among layers. Hexagonal arrays of carbon atoms within a sheet are covalently bonded, and they are sp^2 hybridized to form 0.142 nm sigma bonds with three nearest neighbors in the sheet. The EG was prepared in a manner similar to that reported in the literature (21, 22). Briefly, graphite flakes were first oxidized in a solution of concentrated sulfuric acid and nitric acid, which had a volume ratio of 4:1, for 48 h. The acid-treated graphite flakes were washed with distilled water until the pH was approximately 5–6, and then dried at 100°C to remove the remaining water. The dried graphite flakes were heated at 1,000°C for 30–60 s. The EG thus obtained had c-direction expansions of more than a hundred fold.

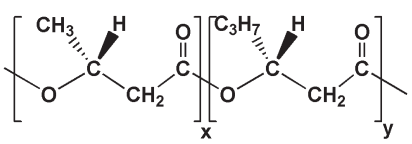

Fig. 1. Molecular structure of poly(3-hydroxybutyrate-*co*-3-hydroxyhexanoate).

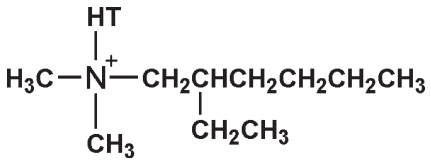

Fig. 2. Chemical structure of the cation used in clay25A, where HT is hydrogenated tallow (~65% C18, ~30% C16, ~5% C1).

2.3 Sample Preparation

PHBHx/clay25A nanocomposites and PHBHx/EG nanocomposites were prepared by melt extrusion. First, various ratios of PHBHx and clay25A (100/1, 100/3, 100/5, 100/7) (designed as NC1, NC3, NC5, NC7, respectively) and various ratios of PHBHx and EG (100/1, 100/2, 100/4, 100/6) (designed as NG1, NG2, NG4, NG6, respectively) were separately mixed in a Brabender mixer for at least 15 min at 150°C. The composites were then thermally compressed into 1 mm thick films using a standard hot press, to yield samples for studies of morphology and determinations of various properties.

2.4 Characterization

2.4.1 Wide-angle X-ray Diffraction (WAXD)

WAXD patterns of neat PHBHx, clay25A, EG and the corresponding composite films were obtained using an X-ray generator (a Siemens D500 diffractometer) (monochromatized Cu-Kα radiation, with 30 mA, 40 kV, $\lambda = 1.5406$ Å). Data were collected with a 2θ scan range of 2 to 20° at room temperature with a step size of 0.05 degree, and a time per step of 1 s.

2.4.2 Transmission Electron Microscopy (TEM)

TEM images were obtained using a JEM 1230 EX-II instrument (JEOL, Tokyo, Japan) operated with 1×10^4 magnification at an acceleration voltage of 80 kV. The ultrathin sections (less than 200 nm) had been microtomed using a Super NOVA 655001 instrument (Leica) with a glass knife and were then subjected to TEM observation without staining.

2.4.3 Strain-stress Measurements

The values of the modulus, tensile strength, elongation at break, and toughness of the samples having dimensions of $30 \times 5 \times 1\ mm^3$ were measured at 25°C using a fully computerized Instron mechanical tester (Model 1122, Acton, MA) at a crosshead speed of 5 mm/min with the initial gauge length being 20 mm. The tensile properties, including Young's modulus and tensile strength at break, were determined for each sample as an average of at least five tests.

2.4.4 Thermogravimetric Analysis (TGA)

TGA was performed using a TA Instruments (TGA 2050 Thermogravimetric Analyzer) with nitrogen as purging gas (30 ml/min) by increasing the temperature from room temperature to 450°C at a heating rate of 20°C/min.

2.4.5 Differential Scanning Calorimetry (DSC)

DSC measurements of the nanocomposites were performed with a TA Instruments (DSC 2010) with nitrogen as purging gas (30 ml/min) over a temperature range from −25 to 200°C at a heating rate of 10°C/min. The samples used for the DSC measurements were the same as those for the WAXD analysis.

2.4.6 Electric Conductivity Measurements

Electrical conductivity was measured using a Keithley 8009 test chamber combined with a 6517A electrometer using sheets (Fig. 3a). Lower resistivity samples were measured using a 4-point fixture combined with a Keithley Digital multimeter 2000 electrometer (shown in Fig. 3b) with different text fixtures: text fixture 8009 for sheets d = 600 nm, thickness up to 1 mm; text fixture 8002A for filaments, strands and molded specimens; home-built unit for strip samples (ca. $40 \times 5 \times 1$ mm) on strips (3×20 mm) cut from the sheets. Strips were usually cut from the sheets and measurements were made along the strip by means of a home-built sample fixture in combination with a digital multimeter.

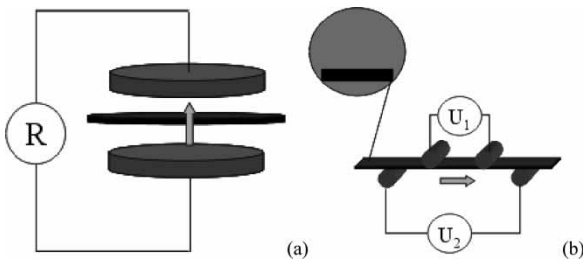

Fig. 3. The setup used to measure electrical volume resistivity: (a) for high resistivity and (b) for low resisitivity.

3 Results and Discussion

3.1 Extent of Clay and EG Dispersion

The WAXD patterns for the neat PHBHx, the clay25A, and their corresponding composites in the range of $2\theta = 2 \sim 20^\circ$ are presented in Fig. 4(a). These results are consistent with known structural features, as summarized below. Each nanolayer of this smectite clay consisted of two tetrahedral sheets (mainly Si and occasionally Al) and a central octahedral sheet (occupied by Mg, Al, etc.), with a lateral dimension of 0.2–2 μm and a thickness of about 1 nm. The stacking of nanolayers forms tactoids (similar to crystallites) that are typically 0.1–1 μm thick (23). This layered silicate exhibits a net negative charge on the lamellar surface, which enables it to absorb cations, such as Na^+ or Ca^{2+}, and occupies the gallery space between nanolayers in the naturally occurring mineral. Because the negative charge originates in the silicate layer, the cationic head group of the alkylammonium molecule preferentially resides at the layer surface going from hydrophilic to organophilic. Additionally, the organic cations can contain various functional groups that react with the polymers and improve adhesion between the reinforcement particles and the

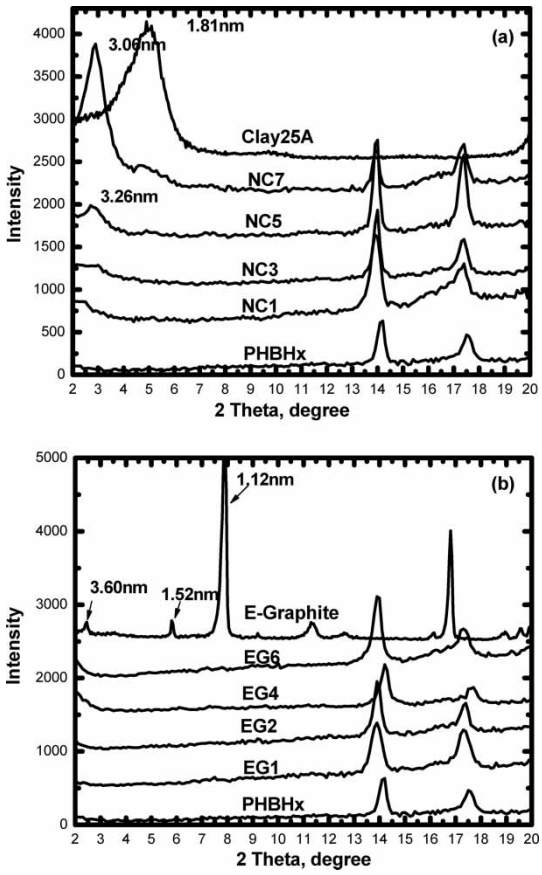

Fig. 4. X-ray diffraction patterns for neat PHBHx, layered-silicate clay25A, and PHBHx/layered-silicate nanocomposites (a) and EG nanocomposites (b) at various loadings.

matrix, thus producing nanocomposites with high dispersion in organic solvents. Natural Na^+-clay has also been extensively used for nanocomposites via the emulsion polymerization method (24, 25). The alkylammonium molecule structure used in clay25A is shown in Fig. 2. The WAXD results bear on the regular arrangements of silicates layers in intercalated forms, and the irregular arrangements in the case of complete exfoliations of the layers. As usual, the 2θ values can be converted to layered spacing d values through the Bragg relationship ($\lambda = 2d\sin\theta$), where λ is the wavelength of the radiation. The interaction of alkylammonium cations with clay usually increases the interlayer spacing relative to that of the pure clay, leading to a shift in X-ray diffraction peak toward a lower angle. The d spacing of the original clay25A expanded to 1.81 nm.

The pattern of the neat PHBHx is displayed as a baseline to compare the existence of diffraction peaks coming from layered silicate dispersed in the matrix. The peak of the neat PHBHx at 13.9° corresponds to the crystallites in the matrix. The interaction of polymer chains with the alkylammonium cation on the surface of clay usually also increases the interlayer spacing relative to that in the original clay. The finite layer expansion associated with intercalated structures resulted in a new basal reflection that corresponded to the layer gallery height of the intercalated nanocomposites. The d spacing of the clay expanded significantly, from 1.81 nm to 3.06 nm for NC7 and 3.26 nm for NC5. It is also clear that the intensities of the WAXD peaks almost disappear in NC3 and NC1, which means that there is no intercalated structure in the matrix.

The X-ray diffraction (XRD) patterns for the series of neat PHBHx, the EG, and their corresponding composites in the range of $2\theta = 2 \sim 20°$ are presented in Fig. 4 (b). As for the WAXD pattern of the pure EG, there were a sharp (001) peak at $d = 1.12$ nm ($2\theta = 7.90°$) and some other peaks with less intensity at $d = 3.604$ nm ($2\theta = 2.42°$) and $d = 1.52$ nm ($2\theta = 5.81°$), which means that EG has multiple ordered platelet structures. It is suggested that, as shown in Fig. 5, after oxidization with concentrated sulfuric acid and nitric acid, and heating at high temperature, many polar groups such as hydroxyl, carboxyl etc. were introduced onto the surface of the graphite. This gave the expansion in c-direction and led to the peak moving to lower angles in the WAXD results. Fig. 4 (b) also shows that there is no peak in the WAXD results for NG1, NG2, NG4, and NG6, which clearly indicates that there is almost no ordered EG in the matrix. It thus suggests that the EG was extensively exfoliated into disordered layers. The unusual peak shown here suggests the existence of PHBHx crystallites in the nanocomposites.

The internal nanometer-scale structure was also studied by TEM, which provides direct visualization of the morphology, atomic arrangement, spatial phase distribution, and structural effects of a selected sample area. Figure 6 shows the TEM images of the PHBHx nanocomposites (a) NC3, (×6,000), (b) NC3 (×10,000), (c) NG2 (×6,000), and (d) NG2 (×10,000). The dark entities in Figs. 6 (a) and (b) are

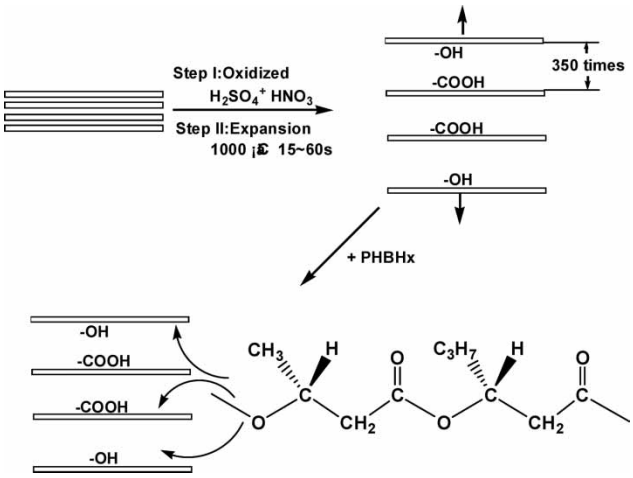

Fig. 5. Expanded graphite preparation and interaction with PHBHx.

exfoliated clay layers. From the TEM results, it is clear that stacks of the clay25A layers are extensively dispersed and exfoliated into layers in the polymer matrix although groups of ordered platelets may form upon increase in the amount of clay loaded (26). The WAXD results thus indicate that the clay is well exfoliated into sheets that should reinforce the polymers. It is supposed that the interaction between the alkyl chains or the tallow chains on the quaternary ammonium compound and the polymer chains may help to improve compatibility, and force the polymer chains to intercalate into the layers, leading to exfoliation of the clay during melt blending.

From the TEM results in Figs. 6 (c) and (d), the dark entities are EG layers. It is obvious that the EG is further dispersed and exfoliated into layers in the polymer matrix even when the parts per hundred loading of EG was increased to 100/6. It is known that after oxidation with concentrated sulfuric acid, some functional groups such as hydroxyl, carbonyl and ether groups embedded in carbon sheets in EG lamella make graphite hydrophilic, and also produce strong interactions. This readily leads to insertions of polar polymers, and also enables it to exhibit rich interaction chemistry, as shown in Fig. 5. This would easily lead to insertion of polar polymers into lamellae to form intercalated or even exfoliated nanocomposites. These results suggest the presence of strong molecular forces between the EG and the polymer chains, such as hydrogen bonding and Coulombic forces (14). Similar results were found for the system based on EG and polymers such as Nylon 6 (27, 28), poly(ethylene oxide) (29), poly(vinyl alcohol) (30), poly(vinyl acetate) (14), poly(diallyldimethylammonium chloride) (31), even poly(furfuryl alcohol) (32), and several others (33).

3.2 Effect of Layered Fillers on the Crystallinity of Matrix

As can be seen in the WXRD results shown in Fig. 4, the crystalline part of PHBHx is characterized by a broad maximum

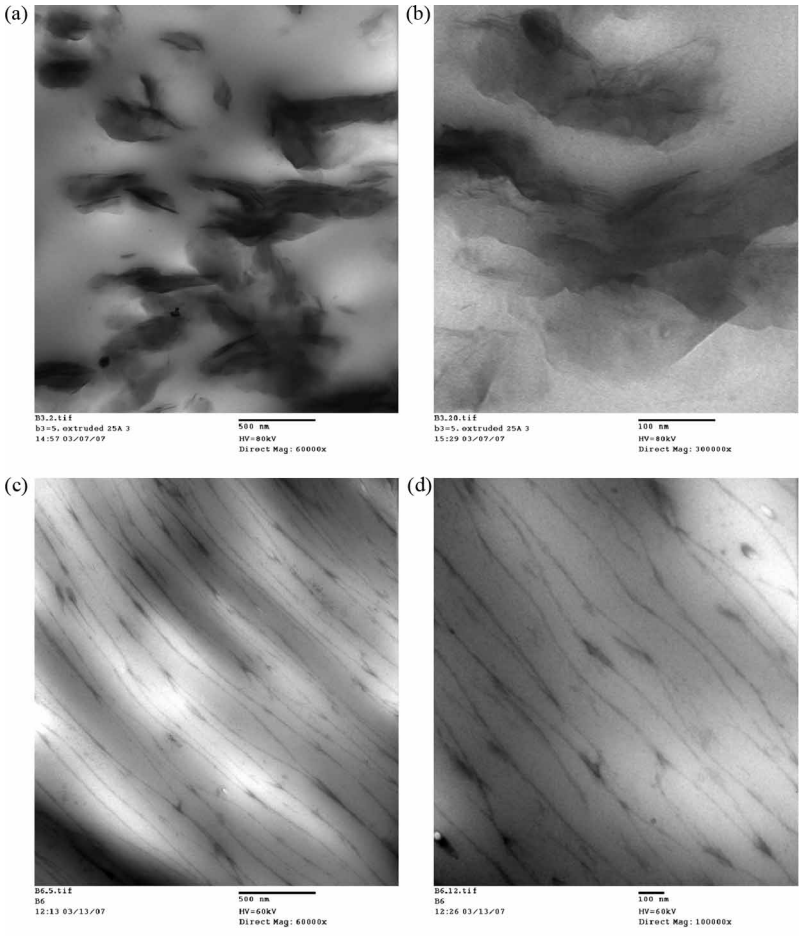

Fig. 6. TEM images of PHBHx nanocomposites: (a) NC3, ×6,000, 500 nm scale; (b) NC3, ×10,000, 100 nm scale; (c) NG2, ×6,000, 500 nm scale; and (d) NG2, ×10,000, 100 nm scale.

located around $2\theta = 20^\circ$, whereas the crystalline zones display two diffraction peaks near 14° and 17.5°. According to the DSC results in Fig. 7, there are two melting temperatures (around 136 and 152°C) and two glass transition temperatures (around 0 and 50°C) for the pure PHBHx. These values agree with the results reported for poly(3-hydroxybutyrate-co-3-hydroxyhexanoate) (34). The appearance of intermediate states of PHBHx has been suggested by a small but wide endothermic pre-melting peak around 60°C in the DSC results. The present DSC results for the PHBHx do show the peak around 60°C for the bulk samples, which agrees with results reported elsewhere (34–36).

The DSC curves for the NC series and the NG series of nanocomposites are shown in Figs. 7 (a) and (b), respectively. It is clear that the two glass transition temperatures of PHBHx are only slightly affected by the exfoliated clay in the matrix. However, the two melting peaks, especially the peak near 136°C, are broadened compared with those of the neat PHBHx. That is, the incorporation of the exfoliated clay increased the melting temperature of the polymer, and this is consistent with results reported by Chen (37). The exfoliated clay may act as the heat barrier that retards the transfer of heat to melt the crystallites in the polymer, and this leads to an apparent higher melting temperature.

As shown in Fig. 7 (b), the same trend was observed in the NG series of nanocomposites. That is, the glass transition temperatures were only slightly affected by the incorporation of EG. However, the melting peaks were also broadened with increasing amounts of EG in the polymer matrix. It is suggested that the polar groups on the surface of the EG may increase compatibility with the matrix, and the surface may provide nucleation centers for lamellar growth (38).

3.3 Thermal Stability

The TGA results for the NC and NG series of nanocomposites are shown in Figs. 8 (a) and (b), respectively. The onset of thermal degradation point was taken to be the temperature at 5% weight loss. There was a decrease in the onset of thermal degradation temperature with increasing amount of dispersed silicate layers. The onset of thermal degradation temperature decreases up to approximately 22°C in the NC series, compared with that of the neat PHBHx. The residual weight, calculated as the weight at 320°C, of course increases

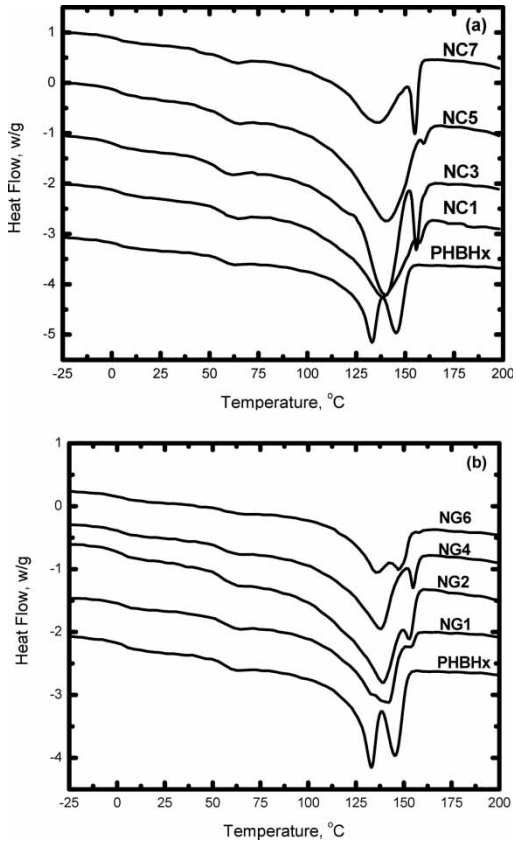

Fig. 7. DSC curves for neat PHBHx, (a) PHBHx/clay25A nanocomposites, and (b) PHBHx/EG nanocomposites.

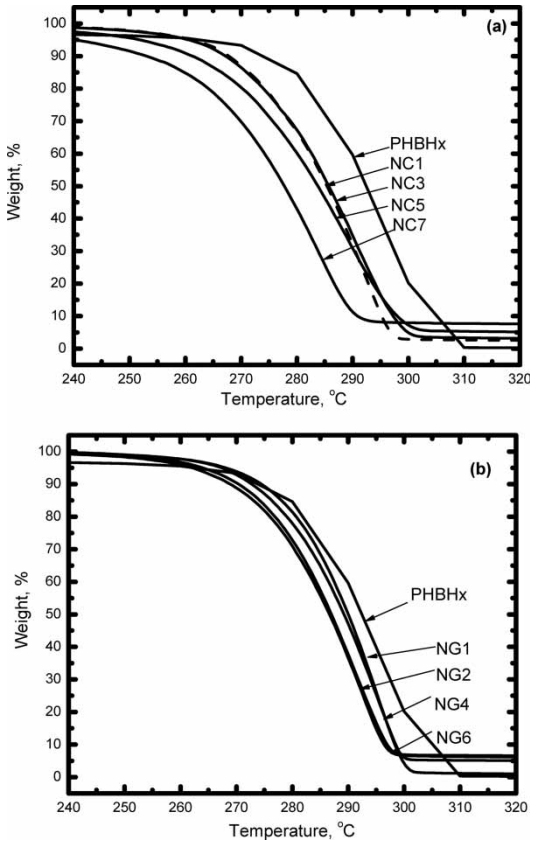

Fig. 8. Thermal stabilities of the nanocomposites based on PHBHx with clay25A (a) and EG (b).

with the increasing amount of clay; it was, however, not proportional to the amount of clay incorporated. This could be explained by assuming that the addition of clay enhanced the performance by acting as a superior insulator and mass-transport barrier to the volatile products generated during decomposition. At the same time, a small amount of clay may also restrict thermal motion of the polymer on the surface of the silicate layers, which is actually the absorbed or chemically bonded polymer matrix on the surface of the layered fillers (39). Therefore, the residual weights are also somewhat more than the corresponding amount of layered fillers incorporated. This kind of improvement in thermal stability was also observed in other systems, such as the intercalated nanocomposites prepared by emulsion polymerization (24).

As shown in Fig. 8 (b), similar trends were observed for the onset thermal degradation temperature, and the residual weight at 320°C for the NG series. However, the onset of thermal degradation temperature decreased up to about 10°C compared with that of the neat PHBHx. This could also be explained by the fact that the fine dispersion of EG in the PHBHx matrix, the strong physical and chemical interactions between EG and PHBHx, and the heat conductivity of graphite layers may help to transfer the heat inside, which would lead to less heat accumulation for degradation than in the NC series.

3.4 Mechanical Properties

The reinforcement by clay or EG in PHBHx is illustrated by values of the Young's modulus, tensile strength (defined as the stress at break), toughness, and elongation at break, as shown in Fig. 9. The Young's modulus, presented in Fig. 9 (a), was greatly improved compared to that of the neat PHBHx, especially at very small loadings (less than 100/3) of organoclay or EG. However, the Young's modulus decreased somewhat with increasing layered filler content when the amounts of the layered fillers was over 100/3. The improvement of Young's modulus by EG is higher than that obtained using the corresponding amount of clay25.

The tensile strength increased a little with increasing loadings of the exfoliated clay or EG when the amount of layered fillers was less than 100/1, as shown in Fig. 9 (b). However, the tensile strength of the NC series decreased when the amount of layered silicate was over 100/1 and again increased slightly when the amount of clay25A was over 100/4. The tensile strength in the NG series decreased when the amount of EG was over 100/1.

There is an obvious trend of decreasing toughness of the NC and NG series with increasing filler concentration, as shown in Fig. 9 (c). The elongation at break of the NC and NG series increased slightly at contents less than 100/1 and decreased with increasing layered fillers when the content

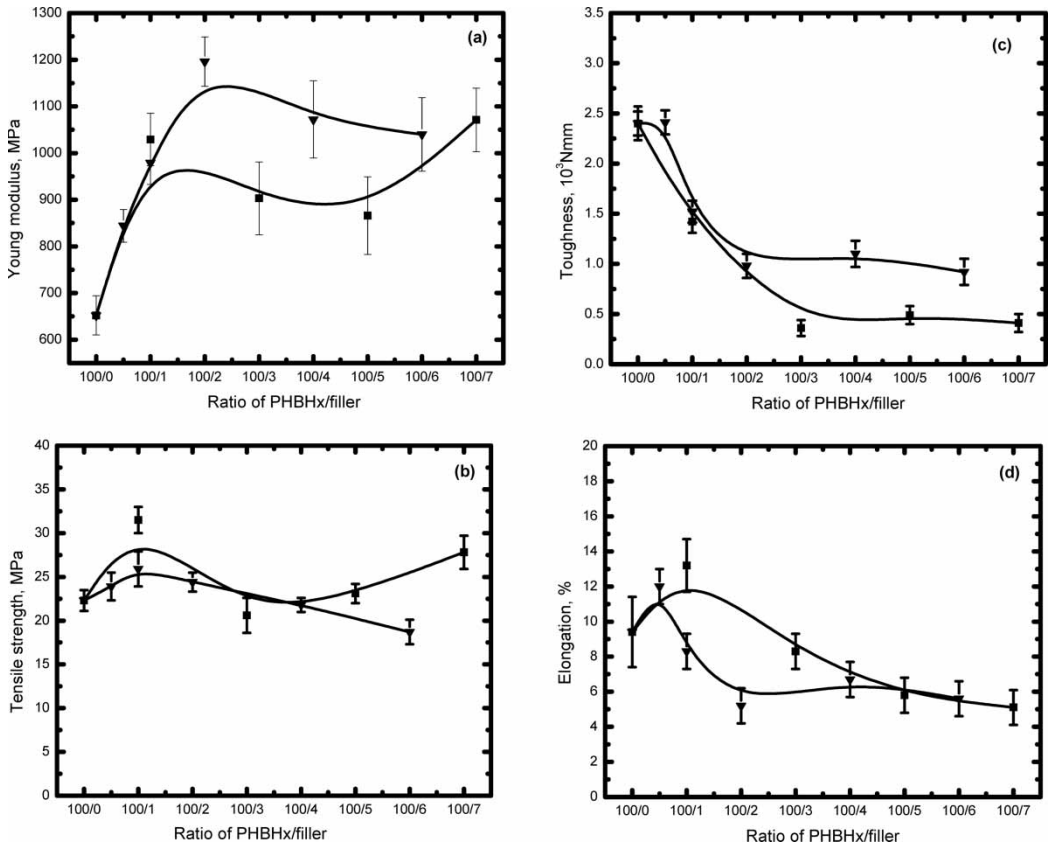

Fig. 9. Young's modulus (a), tensile strength (b), toughness (c) and elongation at break (d) of nanocomposites based on PHBHx with layered silicate clay25A (-■-) and EG (-▼-).

was larger than 100/1, as shown in Fig. 9 (d). The fine dispersion of layered fillers in the matrix may decrease the chains' mobilities during tensile extensions. Recently, a reduction in elongation at break with increasing layered silicate content was also reported for thermoplastic/layered silicate systems (40).

3.5 Conductivity of PHBHx/EG

As shown in Fig. 10, the resistivity of the NG series is still in the range $10^{15} \sim 10^{16}$ Ohm-cm with the amounts of EG used to improve the other properties of this nanocomposite. Since materials with resistivity values lower than 10^4 Ohm-cm can be regarded as electrically conductive materials, the PHBHx/EG nanocomposites with filler content less than 100/10 would not be in this category at present.

The electrical conductivity of EG/polymer nanocomposites is strongly related to filler-filler networking in the polymer matrix, which depends on the nature of the particle dispersion, the EG particle sizes, the amount of the EG, and processing condition during extrusion blending and hot compression. EG consists of sheets, which should be favorable in giving low values of the percolation threshold concentration necessary for conducting pathways. At the same time, numerous other research studies also concluded that the electric conductivity of hybrid systems are strongly related to the conditions used in the preparation and mixing procedures applied (41–43), and to the temperature and hydrostatic pressure during sheet formation (44). However, the TEM results clearly showed that the successful achievement of nanoscale dispersions of EG in PHBHx, which also showed that the sheets are completely separated from each

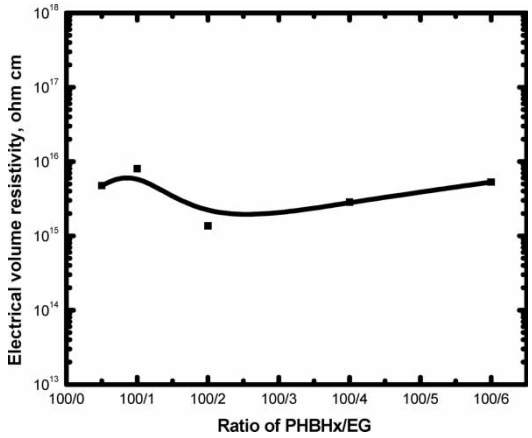

Fig. 10. The electrical volume resistivity of the PHBHx/EG composites as a function of composition.

other, which seems reasonable to expect the high resistivity values. Potschke's results (41) also demonstrated that the resistivity value less than 10^4 Ohm-cm could only be reached in polycarbonate/EG nanocomposites when the EG content was over 17.5 wt% prepared under certain conditions. In the case of the present system, future work should be carried out for the conversion of such EG dispersions to ones yielding filler-filler networks that show electrical conductivity.

4 Conclusions

Novel nanocomposites based on the biodegradable polyester PHBHx and layered silicate clay 25A or EG, were successfully prepared by melt blending. The WAXD and TEM results clearly demonstrated that the clay 25A and EG were exfoliated in the polymer matrix, especially at low filler contents. The major benefit was the considerable increase in the Young's modulus and tensile strength of PHBHx/clay 25A and PHBHx/EG nanocomposites, particularly at very low filler contents. The introduction of clay 25A and EG decreases the onset thermal degradation temperature and increases the thermal degradation rate of the PHBHx. The exfoliated state of EG in the PHBHx matrix does not help to form the filler-filer network to make the NG nanocomposites electrically conductive at the loadings used to improve other properties of these materials. Further research in the effect of exfoliated clay and EG on the biodegradability of these interesting and important materials is ongoing, with some of the focus being on electrical conductivity, biodegradation mechanisms, chemical syntheses, and additional mechanical properties (45–48).

5 Acknowledgments

It is our pleasure to acknowledge the financial support provided JEM by the National Science Foundation through grant DMR-0314760 (Polymers Program, Division of Materials Research), and some help with the XRD measurements in the Department of Geology, The University of Cincinnati.

6 References

1. Chen, B. and Evans, J.R.G. (2006) *Macromolecules*, **39**, 747.
2. Ray, S.S., Yamada, K., Okamoto, M. and Ueda, K. (2002) *Nan. Lett.*, **2**, 1093.
3. Lin, G., Tian, M., Lu, Y.L., Zhang, X.J. and Zhang, L.Q. (2006) *Polym. J.*, **38**, 498.
4. Noda, I. (2000) Absorbent articles comprising biodegradable PHA copolymers. US. Pattent 6,160,199 Dec. 12 2000.
5. Tian, G., Wu, Q., Sun, S.Q., Noda, I. and Chen, G.Q. (2002) *J. Polym. Sci. Part B: Polym. Phys.*, **40**, 649.
6. Satkowski, M.M., Melik, D.H., Autran, J.P., Green, P.R., Noda, I. and Schechtman, L.A. *Biopolymers*; Wiley-VCH: Weinheim, 2001.
7. Noda, I., Green, P.R., Satkowski, M.M. and Schechtman, L.A. (2005) *Biomacromol.*, **6**, 580.
8. Venkitachalam, R., Mark, J.E. and Noda, I. (2005) *J. Appl. Polym. Sci.*, **95**, 1519.
9. Hassan, M.K., Abdel-Latif, S.A., El-Roudi, O.M., Sharaf, M.A., Noda, I. and Mark, J.E. (2004) *J. Appl. Polym. Sci.*, **94**, 2257.
10. Hassan, M.K., Abou-Hussein, R., Zhang, X.J., Mark, J.E. and Noda, I. (2006) *Mol. Cryst. Liq. Cryst.*, **447**, 341.
11. Usuki, A., Kojima, Y., Kawasumi, M., Okada, A., Fukushima, Y., Kurauchi, T. and Kamigato, O. (1993) *J. Mater. Res.*, **8**, 1179.
12. Zhang, X., Lin, G., Abou-Hussein, R., Hassan, M.K., Noda, I. and Mark, J.E. (2007) *Europ. Polym. J.*, **43**, 3128.
13. Liu, P.G., Gong, K.C., Xiao, P. and Xiao, M. (2000) *J. Mater. Chem.*, **10**, 933.
14. Stankovich, S., Dikin, D.A., Dommett, G.H.B., Kohlhaas, K.M., Zimney, E.J., Stach, E.A., Piner, R.D., Nguyen, S.T. and Ruoff, R.S. (2006) *Nature*, **442**, 282.
15. Mark, J.E. (2006) *Acc. Chem. Res.*, **39**, 881.
16. Lin, G., Wu, Y.P., Qian, Y.C. and Zhang, L.Q. (2006) *Chinese Synth. Ind.*, **29**, 439.
17. Lin, G., Wu, Y.P., Zhang, X.J., Qian, Y.C., Jia, Q.X. and Zhang, L.Q. (2005) *Chinese Synth. Ind.*, **28**, 1.
18. Zheng, W.G. and Wong, S.C. (2003) *Compo. Sci. Technol.*, **63**, 225.
19. Zou, J.F., Yu, Z.Z., Pan, Y.X., Fang, X.P. and Ou, Y.C. (2002) *J. Polym. Sci. Part B: Polym. Phys.*, **40**, 954.
20. Lin, G., Zhang, X.J., Liu, L., Zhang, J.C., Chen, Q.M. and Zhang, L.Q. (2004) *Europ. Polym. J.*, **40**, 1733.
21. Pan, Y.X., Yu, Z.Z., Ou, Y.C. and Hu, G.H. (2000) *J. Polym. Sci. Part B: Polym. Phys.*, **38**, 1626.
22. Zhou, D.H. (2005) PhD Thesis. University of Cincinnati.
23. Alexandre, M. and Dubois, P. (2000) *Mater. Sci. Eng.*, **R28**, 1.
24. Kim, J.W., Kim, S.G., Choi, H.J. and Jhon, M.S. (1999) *Macromol. Rap. Commun.*, **20**, 450.
25. Kim, J.W., Noh, M.H., Choi, H.J., Lee, D.C. and Jhon, M.S. (2000) *Polymer*, **41**, 1229.
26. Vaia, R.A. and Giannelis, E.P. (1997) *Macromolecules*, **30**, 8000.
27. Chen, G., Weng, W., Wu, D. and Wu, C. (2004) *J. Polym. Sci. Part B: Polym. Phys.*, **42**, 155.
28. Weng, W., Chen, G., Wu, D., Chen, X., Lu, J. and Wang, P. (2004) *J. Polym. Sci. Part B: Polym. Phys.*, **42**, 2844.
29. Wang, W.P. and Pan, C.Y. (2004) *Europ. Polym. J.*, **40**, 543.
30. Matsuo, Y., Hatase, K. and Sugie, Y. (1998) *Chem. Mater.*, **10**, 2266.
31. Kotov, N.A., Dekany, I. and Fendler, J.H. (1996) *Advan. Mater.*, **8**, 637.
32. Kyotani, T., Moriyama, H. and Tomita, A. (1997) *Carbon*, **35**, 1185.
33. Kovtyukhova, N.I., Ollivier, P.J., Martin, B.R., Mallouk, T.E., Chizhik, S.A., Buzaneva, E.V. and Gorchinskiy, A.D. (1999) *Chem. Mater.*, **11**, 771.
34. Sato, H., Nakamura, M., Padermshoke, A., Yamaguchi, H., Terauchi, H., Ekgasit, S., Noda, I. and Ozaki, Y. (2004) *Macromolecules*, **37**, 3763.
35. Tian, G., Wu, Q., Sun, S., Noda, I. and Chen, G.Q. (2001) *Appl. Spectrosc.*, **55**, 888.
36. Wu, Q., Tian, G., Sun, S., Noda, I. and Chen, G.Q. (2001) *J. Appl. Polym. Sci.*, **82**, 934.
37. Chen, G.X., Hao, G.J., Guo, T.Y., Song, M.D. and Zhang, B.H. (2004) *J. Appl. Polym. Sci.*, **93**, 655.
38. Tracz, A., Jeszka, J., Kuciska, I., Chapel, J.-P. and Boiteux, G. (2001) *Macromol. Symp.*, **169**, 129.

39. Daly, P.A., Bruce, D.A., Melik, D.H. and Harrison, G.M. (2005) *J. Appl. Polym. Sci.*, **98**, 66.
40. Lim, S.T., Hyun, Y.H., Choi, H.J. and Jhon, M.S. (2002) *Chem. Mater.*, **14**, 1839.
41. Potschke, P., Abdel, G.M., Pegel, S., Mark, J.E. and Heinrich, G. (2003) *Polym.Prep.*, **43**, 760.
42. Nagata, K., Iwabuki, H. and Nigo, H. (1999) *Comp. Inter.*, **6**, 483.
43. Abdel-Goad, M., Potschke, P., Zhou, D.H., Mark, J.E. and Heinrich, G. (2007) *J. Macromol. Sci. Part A-Pure & Appl. Chem.*, **44**, 591.
44. Celzard, A., Mcrae, E., Mareche, J.F., Furdin, G. and Sundqvist, B. (1998) *J. Appl. Phys.*, **83**, 1410.
45. Doi, Y., Kitamura, S. and Abe, H. (1995) *Macromolecules*, **28**, 4822.
46. Kobayashi, G., Shiotani, T., Shima, Y. and Doi, Y. *Biodegradable Plastics And Polymers*; Elsevier: Amsterdam, 1994.
47. Abe, H., Doi, Y., Aoki, H. and Akehata, T. (1998) *Macromolecules*, **31**, 1791.
48. Kunioka, M., Tamaki, A. and Doi, Y. (1989) *Macromolecules*, **22**, 694.